INFLUENCE OF A SURFACE FRICTION ON THE DEFORMATION PROCESS OF RING MADE OF NONLINEAR PROPERTIES MATERIAL

Tadeusz Wegner

Poznan University of Technology
Piotrowo 3 Street, 60-965 Poznan
e-mail: tadeusz.wegner@put.poznan.pl

Marek Kokot

University of Zielona Gora, Faculty of Mechanical Engineering
Prof. Z. Szafrana 4 Street, 65-516 Zielona Góra
tel.: +48 68 3282950
e-mail: m.kokot@iizp.uz.zgora.pl

Abstract

The paper presents application of an energy-based finite element and a local relaxation method to computer calculation of deformation of a ring made of hyperelastic material. The present study considers a surface friction mechanism. This mechanism is a physical phenomenon counteracting the relative motion of the contacting bodies. Friction causes loss of energy the dissipation of which is a result of wearing out of the bodies' surfaces and heat emission. This directly affects the shape of the deformed body. The above statements are confirmed by the results of computer calculation performed for rubber ring with rectangular cross-section. Rubber is a nearly incompressible material and, therefore, requires application of special mechanical models of the material properties as well as proper calculation methods. Implementation of energy-based finite element and local relaxation method enables studying the ring deformation with consideration of nonlinear properties of rubber and its displacements in the plate-ring contact plane, according to the value of a friction coefficient between rubber and the plate material. Application of energy method resulted in determination of the work of friction forces and the energy density distribution of volumetric and deviatoric strain. It also simplified energy analysis of the surface friction mechanism and influence of the friction coefficient value on the process of the ring deformation.

Keywords: hyperelastic material, surface friction, energy methods, energy-based finite element

1. Energy-based finite element

The analyses making use of the energetic methods enable describing the processes that undergo in three-axial stress state and interpreting the phenomena in the energetic approach. The energetic methods may be used for researching such phenomena as plastic flow [10-12, 15, 16], cracking or material fatigue. The energetic models of material use the notion of the strain energy of the material [8-25] and appropriate material constants modelling the material properties, according to the state of deformation. In the classic Finite Element Method the relationships between displacements of the nodes and the forces acting thereon are expressed with the help of the element stiffness matrix. On the other hand, in an energetically modelled finite element [8, 16, 22-25] the stiffness matrix is not necessary. Thanks to the use of the strain energy function instead of the classical constitutive equation of the material in order to describe mechanical properties of the material, an energetically modelled finite element has been developed. It allows determining the energy of the element deformation according to displacement components of the nodes.

Deformation of the body induces the growth of the energy due to the deformation. The strain energy of the body related to its volume in undeformed state is described by the function of the

density of the strain energy U. It depends on the condition of body deformation. Therefore, for an isotropic material the function is expressed in terms of the invariants of the state of deformation I_1, I_2, I_3:

$$U = U(I_1, I_2, I_3), \tag{1}$$

that guarantees that its value does not depend on the choice of the direction of coordinate system axes.

Behaviour of an isotropic incompressible solid was described for the first time by Mooney, who in 1940 presented the density function of the strain energy in the following form, assuming linear relationship between the stresses and deformations:

$$U(I_1, I_2) = C_1(I_1 - 3) + C_2(I_2 - 3), \tag{2}$$

where C_1, C_2 are material constants to be experimentally determined.

Nevertheless, it has appeared that the function given by the formula (2) describes satisfactorily only the behaviour of the caoutchouc-like material. Such a material is nearly incompressible and, therefore, its volume remains nearly constant while loading and unloading, as compared to the initial volume. Meantime, the ideally incompressible materials do not exist, since every material is characterized by certain compressibility. Therefore, the incompressible material might be considered only as a simplification. In consequence, the considered material shall be assumed to be nearly incompressible. As an example of such a material the rubber may be mentioned.

Assuming that every material is compressible to a certain degree, the calculation for the materials of nonlinear properties, among which the rubber may be reckoned, is made based on a modified Mooney function. The modified function takes a form [8]:

$$U = C_1(I_1 - 3\sqrt[3]{I_3}) + C_2(I_2 - 3\sqrt[3]{I_3^2}) + \frac{1}{2}K\frac{(\sqrt{I_3} - 1)^2}{\sqrt{I_3}}, \tag{3}$$

where K is the module of volumetric deformation. Sufficiently big K value means that the relationships so obtained characterize nearly incompressible material. Modification of the Mooney model consists in addition of a third component based on the I_3 invariant, equal to square of the relative volume of the material (8). This component represents specific energy of the volumetric strain U_V. The I_1 and I_2 invariants occurring in the Mooney formula (2) have been so corrected [8, 9, 16] as to ensure that two first components of the formula (3) describe the specific energy of the pure deviatoric strain U_S. Modification of the function (2) is aimed at improving accuracy of the energetic model of the material. Literature provides various energetic models of the hyperelastic materials [16, 23]. Their choice depends on material properties and the selected material should possibly accurately reflect actual physical relationships existing between the stresses and deformations of the three-axial stress state.

The modified Mooney function (3) has been used for formulation of an energy-based finite element in the form of a ring with rectangle cross-section, shown in Fig. 1.
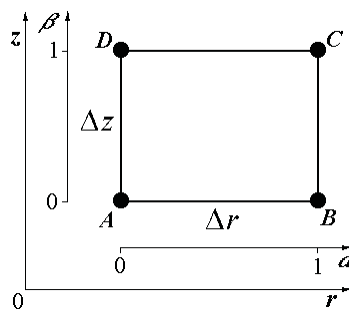

Fig. 1. Axisymmetrical finite element in a ring shape with rectangular cross-section and nodes in points A, B, C, D

Density of the strain energy is a function of the invariants of the strain state. The function represented by the formula (3), describing the strain energy of practically incompressible materials, like rubber, enables expressing density of the element strain energy as a function of the components of the nodes displacements and local coordinates α and β:

$$U(u_A, w_A, u_B, w_B, u_C, w_C, u_D, w_D; \alpha, \beta). \tag{4}$$

Integration with regard to the initial volume V of an undeformed element provides the strain energy of a symmetric element of revolution of rectangular cross-section as a function of the components of its nodes displacements [8]:

$$E^{(e)}(u_A, w_A, u_B, w_B, u_C, w_C, u_D, w_D) = \int_V U dV. \tag{5}$$

The energetically modelled finite element considered above has been used for determining the state of displacements of the deformed body with the method of local relaxation, being a calculation method especially developed for this purpose [8] and called so due to local range of the iterations distinguished by relaxation of the body stress.

In the classical approach to the finite element method the stiffness matrix of the element should be determined. In general, the matrix defines the relationship between the components of generalized node displacements in accordance with particular degrees of freedom and the components of generalized forces corresponding to these degrees of freedom. In the local relaxation method the use of stiffness matrix has been cancelled. Determination of the positions of the nodes is restrained only to the area of the elements directly connected to given node (Fig. 2). Every consecutive iteration consists in improving location of a single node exclusively with respect to the nodes located in the nearest vicinity, which are temporarily considered as being totally restrained, with all degrees of freedom blocked. In result they are unable to move in any direction despite being the points of an elastic medium. Local surroundings of a node is illustrated in Fig. 2.
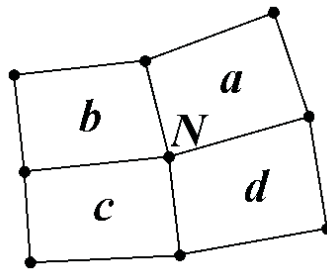

Fig. 2. Local surroundings of a node N

The area surrounding the *N* node is composed of the elements a, b, c, d directly connected to it. The strain energy of the node surrounding area is a sum:

$$E_O = E^{(a)} + E^{(b)} + E^{(c)} + E^{(d)}, \tag{6}$$

where:
E_O - potential energy of the elastic forces of the local surroundings of the node,
$E^{(a)}, E^{(b)}, E^{(c)}, E^{(d)}$ - potential energy of the elements surrounding the node.

Position of the *N* node is improved so as to minimize the potential energy of the elastic forces E_O of the node surroundings. Values of the components of the force of the node interaction with its surroundings is determined based on the increases of the strain energy of the elements directly connected to given node and induced by tentative node displacement in the direction consistent with the degree of freedom corresponding to given force component. Research of energy

variations during node displacements in the direction consistent or opposite with respect to the coordinate axes allows for determining the forces of the node interaction with its nearest surroundings according to the node position. The difference in these forces referred to the node displacement length determines the force gradient being a measure of the local stiffness corresponding to given degree of freedom. The use of local values of the stiffness corresponding to given node enables calculating the new node position suppressing its local imbalance [8]. This procedure is many times repeated for consecutive nodes until the force components of local imbalance of the nodes drop below a given small level.

Detailed mathematical description of the energy-based finite element and the local relaxation method, together with their use for calculation of a rubber ring without consideration of surface friction, is delivered in the following literature items: [8, 13, 16, 20, 22-25]. The works [13, 16, 20, 21] complement the local relaxation procedure so as to enable consideration of the surface friction in the calculation.

2. The friction theories

The technological progress forced the engineers and researchers to analyze the friction phenomenon. We are indebted to famous Leonardo da Vinci for the first analysis of friction. His experiments allowed to state that various bodies have various inclinations to slide. In late 17th Century Amontons published the theory of dry friction. He found that friction is due to climbing of one body against surface irregularities of the other during their motion under the conditions of their normal pressure. He expressed friction with the formula:

$$T = \mu N, \tag{7}$$

where:
T - friction force,
μ - friction coefficient,
N - pressure force.

The formula (7) served as a basis for friction phenomenon and until to-day is used as a basic formula describing the friction. In the literature it is usually referred to as Coulomb model, who published his theory of dry friction in late 18th Century. He described the dry friction phenomenon by the formula:

$$T = \mu N + A, \tag{8}$$

where A is a part of the friction force depending on molecular interaction between both rubbing surfaces.

Industrial development of the 19th Century involved the growth of interest in the friction processes that was conducive to increasing intensity of the researches aimed at describing the process and other accompanying it phenomena. Nevertheless, it appeared quickly that friction is a highly complicated phenomenon, depending on many factors and its occurrence significantly affects durability of cooperating parts. A new domain of science called tribology arose that deals exclusively with researching the friction phenomenon.

Many researchers made efforts with a view to describe the friction phenomenon on various ways. Bowden was one of them. Based on his research he found that the friction coefficient and the type of the damages are determined chiefly in terms of the relative values of physical properties of the rubbing surfaces of solid bodies. On the other hand, according to Epifanov the metal shearing while moving one surface against the other arises not only at the points of actual contact but in the area many times larger than the entire contact surface. Another description of the friction process was delivered by Tomlinson, who stated that friction is a result of adhesive interaction of rubbing surfaces of the bodies while the sum of attractive forces is small and may be ignored. Some researchers try to explain friction by the processes undergoing at the molecular level. The theory developed by Deriagin is based on the assumption that friction is related to

molecular roughness of the body that depends on the material structure. The form and dimensions of the atoms while displacing one body against the other remain constant and, in consequence, the friction process may be presented as overcoming the molecular roughness.

Consideration of all the above theories may lead to conclusion that they all are correct but only to a certain degree. Each of them considers the friction process too unilaterally and, therefore, they do not fully fit the reality. The mechanical theories take, first of all, the cohesion component into account. It means that they mathematically describe the phenomena occurring against the cohesion forces (the elastic deformation, plastic deformation, shearing, etc.). On the other hand, the molecular friction theories are focused on the adhesive interaction and this is the reason why they are unilateral.

The effect of particular mechanical and molecular factors on the course of the friction process is described by the most general tribological law, that says that the friction resistance while displacing two bodies each with respect to the other is equal to the sum of adhesive and cohesive resistance values:

$$T_t = T_{adh} + T_{coh} , \qquad (9)$$

where:
T_t - friction resistance,
T_{adh} - the sum of adhesive resistance,
T_{coh} - the sum of cohesive resistance.

According to the type and conditions of friction the particular components may increase or decrease, or even entirely disappear. For example, in case of external friction between two ideally smooth surfaces the cohesive component is equal to zero. Apart from extreme cases, in which one of the components disappears, there are many indirect cases, in which both, adhesive and cohesive components have significant values.

The resistance due to displacing surfaces is importantly affected by secondary phenomena, as vibration, large heat emission, or electric phenomena. These phenomena, being side effects of friction, cause the growth or reduction of the pressure force between the surfaces, i.e. variation of the adhesive component or cyclical deviations from the equilibrium, i.e. variation of the cohesive component. Taking into account the present state of knowledge their accurate recognition is extremely difficult or even impossible, since these phenomena have a highly dynamical character and vary according to external factors and conditions accompanying the friction. The state of knowledge related to friction, inclusive of rubber friction, is presented in the literature items [1-7].

3. Consideration of surface friction in the method of local relaxation

Friction of elastomers, i.e. rubber first of all, is considered in tribology as a separate phenomenon, due to complicated character of the phenomena occurring there. Elastomers are molding materials distinguished by elasticity of rubber in the temperatures above and below the room temperature. Basic component of elastomers is carbon C12. Elastomer molecules are located in a net of large mesh size. They are obtained by crosslinking (vulcanization) of caoutchouc with the use of crosslinking agents (sulphur, peroxides). Elastomers do not experience large deformations in result of heating or moderate load. Rubber is a product obtained of synthetic caoutchouc. Surface contact causes elastic deviatoric strain. Once the load is released the undeformed state of elastomer is restored. It was found that the strain energy of rubber is dissipated mainly by hysteresis [4]. In case of elastomers the most important part of the friction coefficient is its adhesive component, as opposed to the other polymers. Properties of rubber depend on its chemical composition, duration of its use, conditions of operation, the type and roughness of the surface, etc.

Conditions of cooperation of the rubbing surfaces, when one of them is rubber, depend on high number of factors, among others on chemical composition of rubber, its elasticity and internal structure of the material, outer factors, surface smoothness, the type of the layer, and the substance included between the rubbing surfaces. All these factors are taken into account by properly chosen value of the friction coefficient.

Taking into account the complication of rubber friction the deformation of the rubber ring with consideration of surface friction has been determined with the method based on the energy-based finite element referred to in the first part of the paper, where location of particular nodes of the rubber ring model has been defined with the method of local relaxation.

The main problem consists in formulating the criterion of the conditions in which a given node of the layer adjacent to the plate may move. The pressure exerted on the rubber ring causes the forces that are tangent to the rubbing surfaces, acting crosswise with respect to the ring axis, and the forces normal to the ring compressing plate, acting in parallel to the ring axis (Fig. 3). Knowledge of the shear and normal stresses enables determining the shear and normal forces acting on the surface of the plate-ring contact in the vicinity of the node:

$$N = -\int_A \sigma_z dA, \quad S = \int_A \tau_{zr} dA, \tag{10}$$

where:
N - normal force,
S - shear force,
σ_z - normal stress,
τ_{zr} - shear stress,
A - area of the rubbing surface including the node surroundings before the deformation.

Once the shear force exceeds the maximum value of the friction force depending on the value of the product of the friction coefficient and the normal force, the contact between the rubbing surfaces is broken. What concerns the modelled finite element it leads to unlocking the node located in the area of the shear force. Taking into account high complexity of the friction phenomenon and significant deformability of rubber it was assumed that the upper value of friction force is defined locally based on the Amontons' model of friction, defined by the formula (7) and referred to in literature as the Coulomb model. In order to break the local contact between the rubbing surfaces the following relationship must be met:

$$S > T = \mu N . \tag{11}$$

This leads to local motion of the body along the rubbing surface inducing reduction of the shear stress and changing the normal stress. This, in turn, is conducive to changing the shear and normal forces (10) and, in consequence, inverting direction of the inequality of the condition (11). It means repeated locking of the node displacement. Detailed analysis of the friction process is shown in the work [13]. Based on it the work of the friction mechanism has been expressed in the form of an original computer program developed by the authors of the paper and designed for computation of deformations of a rubber ring with consideration of the friction undergoing at the contact surface between compressed plates (Fig. 3). Consecutive iterations aimed at finding the state of equilibrium of the ring nodes are carried out in accordance with the method of local relaxation until achieving the condition when the quotient of the sum of absolute increments of the displacement components of all the nodes of given iteration to the value of the sum from the former iteration decreases below 1 promille:

$$\frac{\sum_{m=1}^{369}\left(\left|\Delta u_m^{(i+1)}\right| + \left|\Delta w_m^{(i+1)}\right|\right)}{\sum_{m=1}^{369}\left(\left|\Delta u_m^{(i)}\right| + \left|\Delta w_m^{(i)}\right|\right)} \leq 0.1\%, \tag{12}$$

where Δu, Δw - increments of displacement components of the nodes.

4. Energy conservation law in energetic description of the surface friction phenomenon

Thanks to the use of the energetic method one is able to determine the values of the forces acting on the ring. In order to determine the force loading the ring the strain energy increments in particular steps of the increment method are used. The thesis [8] provides comparison of the results obtained with the energetic method and the method making use of the stress values acting on the plate surface. The results so obtained were nearly identical. Nevertheless, the use of the energetic method based on the increments of the ring strain energy is much easier. The thesis [8] presents analysis of the rubber ring deformation the surface of which was free of friction between the ring and the plates compressing it. Taking into account the surface friction phenomenon it should be assumed that a part of the energy accumulated in the ring in the presence of the external forces loading it, considered as the active forces, is dissipated by the surface friction forces. In this case the energy is taken by the external passive forces. This phenomenon should be taken into account while determining the compressing force pressing the ring against the plate. The basic condition that must be satisfied is the energy conservation law:

$$\Delta L = \Delta E_P, \tag{13}$$

where:
ΔL - work increment of the external forces,
ΔE_p - increment of the ring strain energy.

Since the work of the external forces equals the sum of the active forces and reactions:

$$\Delta L = \Delta L^{(P)} + \Delta L^{(T)}, \tag{14}$$

the above relationship substituted to formula (13) provides, after transformations:

$$\Delta L^{(P)} = \Delta E_P - \Delta L^T, \tag{15}$$

where:
$\Delta L^{(P)}$ - work increment of the force compressing the ring (the active force),
$\Delta L^{(T)}$ - work increment of the friction force (the passive force).

The increment of the force compressing the plate to the ring is determined from the formula:

$$\Delta L^{(P)} = P_{śr} \cdot \Delta f, \tag{16}$$

where:
$P_{śr}$ - value of average force compressing the ring,
Δf - deflection increment in given ring load step.

Substitution the relationship resulting from the formula (16) to (15) one obtains the value of the force acting on the ring:

$$P_{śr} = \frac{\Delta E_P - \Delta L^{(T)}}{\Delta f}. \tag{17}$$

The above formula enables determining average value of the ring compressing force, both in case of loading and unloading of the ring. Particular attention should be paid to the values of the work and energy increments occurring while loading and unloading. Since the friction force is a passive force of the sense opposite to the direction of displacement of the part of the ring surface, increment of the work of this force is negative, irrespective of the sign of the deflection increment Δf.

Tab. 1. Values of work increase and strain energy increase in relation to values of ring deflection increase

Δf	$\Delta L^{(P)}$	$\Delta L^{(T)}$	ΔE_P
$\Delta f > 0$ (loading)	$\Delta L^{(P)} > 0$	$\Delta L^{(T)} < 0$	$\Delta E_P > 0$
$\Delta f < 0$ (unloading)	$\Delta L^{(P)} < 0$	$\Delta L^{(T)} < 0$	$\Delta E_P < 0$

Values of the work increments of the loading force and the work of the friction force and increments of the ring strain energy are presented in Table 1. While loading the ring the deflection increment is above zero, while unloading it is less than zero.

5. Research result of a rubber ring with consideration of the surface friction phenomenon

The subject of the research was a ring of rectangular cross-section, made of a practically incompressible material. The static load acts in the ring symmetry axis in form of a force perpendicular to a rigid plate. It was assumed that the plate diameter exceeds the external diameter of the deformed ring. Taking into account the ring symmetry with respect to the plane, the calculation is carried out only for the upper half marked in Fig. 3 with red colour. The modelled part of the ring is divided into 40×8 symmetrical energy-based elements of revolution of square cross-section.
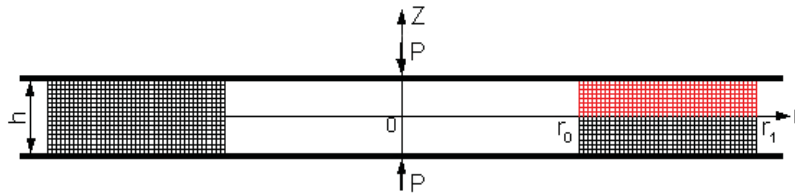

Fig. 3. The rubber ring division into finite elements

The computation was aimed at researching the effect of surface friction on the shape of the ring under compression. The computation consisted in determining deformations of the ring in consecutive intermediate stages – from the undeformed to deformed state, corresponding to the assumed maximal value of deflection of the upper part of the ring. For purposes of the computation for consecutive deflections the Δf increment of the deflection equal to 0.1 mm was assumed. The computation was carried out for the ring assuming the following stationary friction coefficients: $\mu = 0.3$, $\mu = 0.6$ and the ring in which the nodes of its finite elements contacting with the plate are permanently connected with it. In the last case the friction coefficient $\mu = \infty$ was assumed. In all the cases the ring computations have been carried out with the material data corresponding to hard rubber: $C_1 = 1.92$ MPa, $C_2 = 0.08$ MPa and $K=200$ MPa.

In all the figures presenting the obtained results the undeformed ring shapes are marked with red while the deformed ones with black. Around the nodes of the surface layer contacting with the plate the circles are drawn, the colours of which represent the conditions of particular nodes. Blue is for the nodes without displacement. Displaced nodes are marked with red, while the green nodes have been displaced and restrained again.

Analysis of ring shapes of Fig. 4 enables stating that in case of small deflection the differences in the ring deformations are invisible. Nevertheless, more accurate analysis indicates that in both rings where the surface friction phenomenon has been taken into account, several nodes located in the plate-ring contact plane have displaced and, afterwards, restrained again. Such a situation occurred chiefly in the right-hand part of the figure, i.e. nearer to the outer free surface of the ring. Such a character of distribution of the number of displaced nodes is imposed by the fact that the nodes displaced in the ring axis direction (in the figure – the left-hand side) are conducive to decreasing the internal diameter and unit material volume. Taking into account that the assumed material model corresponds to nearly incompressible material, this situation leads to significant growth of the force normal to the surface pressing the material against the plate. Therefore, according to the assumed friction model, the upper friction force increases and the nodes are locked.

Consideration of the number of the displaced nodes (Fig. 4) allows to find that the largest number of the displaced nodes, both in outward and inward directions, occurs in the ring distinguished by small friction coefficient ($\mu = 0.3$). It means that in this case the values of normal forces pressing the ring against the plates were the smallest. This directly determines the range of the work to be done in order to obtain the given ring deformation.
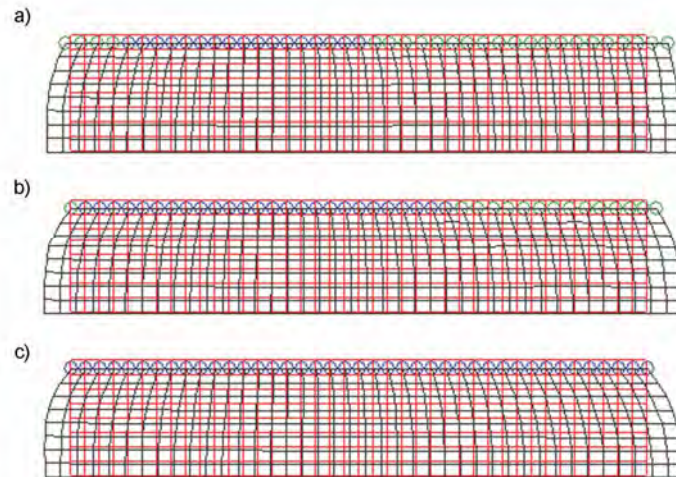
Fig. 4. The ring deformation for deflection f = 0.5 mm and various friction coefficients which were taken into calculations : a) μ = 0.3, b) μ = 0.6, c) μ = ∞
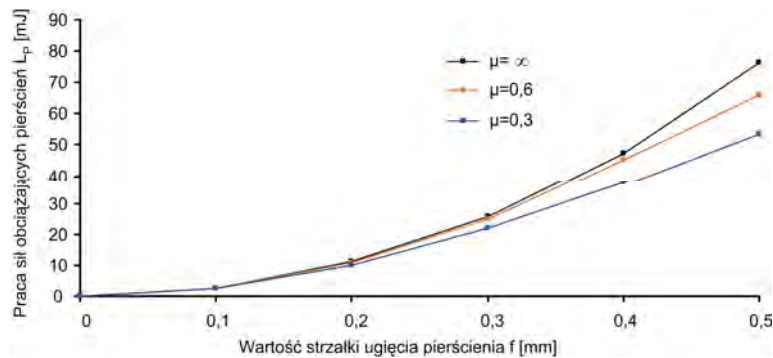

Fig. 5. The work of ring load in relation to its deflection

Figure 5 presents the plots of the work of the ring load force that, according to the formula (15), is a sum of the potential energy of the ring deformation E_P (the work of internal forces) and the energy dissipated in result of the work of friction force equal to L_T. In case of a very small ring deflection the difference in the value of the work of the ring load force for various friction coefficients are minimal. Nevertheless, growth of the deflection results in increase of the difference. According to the plot the smaller friction coefficient used in the computation, the smaller work is performed by the load force of the ring while compressing it to the given deflection.
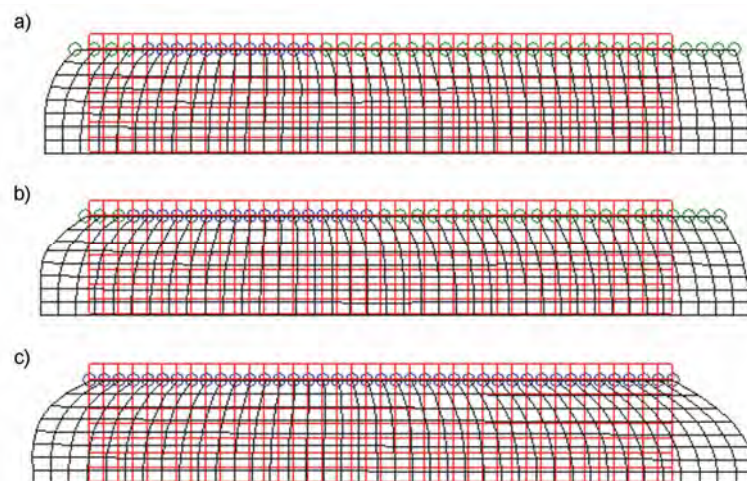

Fig. 6. The ring deformation for deflection f = 1 mm and various friction coefficients which were t aken into calculations: a) μ = 0.3, b) μ = 0.6, c) μ = ∞

Analysis of Fig. 6 presenting the shapes of the rings obtained while deflecting them to the value of 1mm gives evidence of significant differences between them. Convex shapes at internal part of the rings are similar, however, the largest amount of the material is displaced in the ring symmetry plane, the nodes of which located in the plate-ring plane are immobilized. The smallest amount of the material is displaced in case of the ring for which the friction coefficient $\mu = 0.3$ is assumed. Small friction coefficient between the compressing plated and the ring causes unlocking and displacement of larger number of nodes located in the contact plane that is conducive to smaller material flow in the ring symmetry plane. The same mechanism is conducive to differences in convexity at the outer ring side. For higher values of the friction coefficient the number of the nodes unlocked in the plate-ring plane and displaced outward of the ring is smaller and, in consequence, the ring convexity grows.

Figure 7 shows the plots of the work of the ring charging forces. Growth of the friction coefficient causes growing work necessary in order to induce the ring deformation resulting in required ring deflection. Maximal growth is observed in case of the ring marked in the illustration with the friction coefficient $\mu = \infty$, the nodes of which located in the plate-ring contact plane are immobilized.
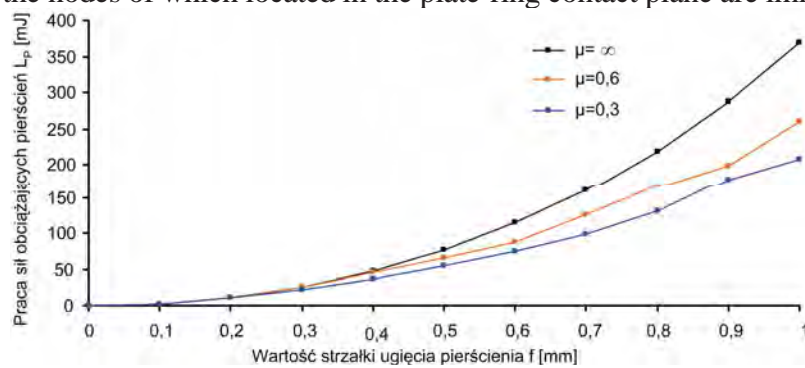

Fig. 7. The work of ring load in relation to its deflection

The results obtained after renewed growth of the ring deflection up to 1.5 mm confirm earlier analyses related both to the obtained final shapes and the work of the ring charging forces. Figure 8 clearly shows how differentiated are ring deformations according to the friction coefficient between the compressing plates and the ring assumed for purposes of the computation. The smallest convexity at the outer side occurred in the ring for which the smallest μ value has been assumed. On the other hand, the highest convexity was found in the ring, whose nodes located in the contact plane were permanently connected with the compressing plate, thus preventing displacement of the ring material in this plane.
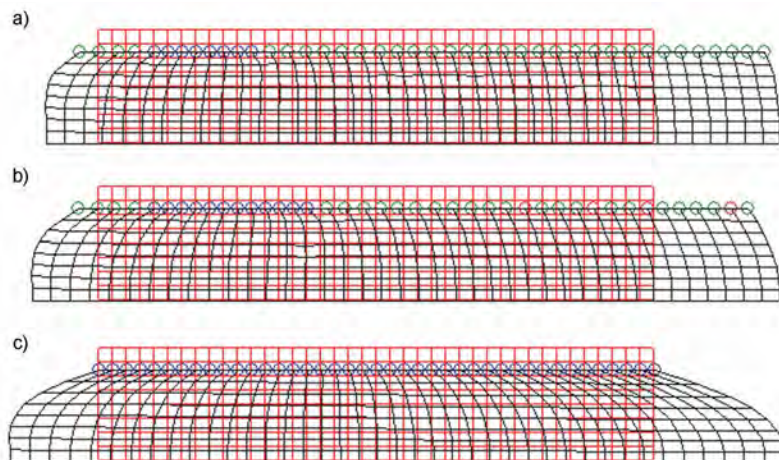

Fig. 8. The ring deformation for deflection f = 1.5 mm and various friction coefficients which were taken into calculations: a) μ = 0.3, b) μ = 0.6, c) μ = ∞

One may notice that greater material displacement outward the ring results in its smaller flow inside the ring in its plane of symmetry. This is due to the need of conservation of balance of the material the ring is made of. Larger rubber outward displacement is compensated by its smaller amount flowing inside. This ensures approximate conservation of the initial amount of material. In case of higher friction coefficient between the compressing plates and the ring, volume of the material that may displace in the contact plane which, in consequence, results in larger material amount outflowing in the ring symmetry plane.

Value of the friction coefficient affects the work of the ring charging forces too. This is evidenced by analysis of the plots shown in Fig. 9. The work to be performed in order to deflect the ring increases with the growth of the deflection itself and with the friction coefficient. Comparison between the rings distinguished by a low and high friction arising between them and the plates allows to state that the work to be performed in order to compress the ring the nodes of which are locked in the contact plane is at least three times as large as in case for which the friction coefficient $\mu = 0.3$ has been assumed.
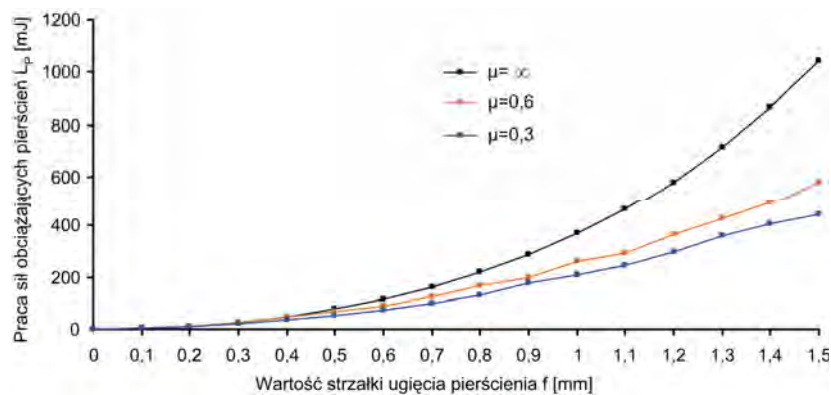

Fig. 9. The work of ring load in relation to its deflection

The shape of the deformed ring and the size of deformation affect distribution of density of the strain energy that may be determined from the formula (3). What is worthy to be noticed is that in reality the shape of the deformed object is determined by the objective energetic criterion that is applied to the iterative procedure of local relaxation aimed at minimizing the strain energy of the object. Precise discussion of the ring energy distribution according to ring deflection would require much more place. Therefore, only the energy distribution of the energy-based finite elements directly adjacent to the compressing plate is discussed. Detailed analysis has shown that just this layer is subject to maximal strain energy.

Figure 10 presents the specific energy distribution of the deviatoric strain U_S that is determined by two first components of the formula (3). Maximal values of the energy arise in the finite elements located the nearest to the outer free part of the ring, the nodes of which are permanently connected to the compressing plate and, in consequence, unable to move in the plane of the plate-ring connection. Taking additionally into account large material displacement in the ring symmetry plane one obtains very high deformation of the finite elements that, in result, lead to huge value of the density of the deviatoric strain energy, which is disadvantageous when considering the strength condition. This problem does not exist in the other two cases, when the nodes in the plate-ring plane contact may freely displace. Material displacement near the plate contact surfaces outward the ring cause smaller deformation of the material and, in consequence, smaller cumulation of the deviatoric strain energy.

Figure 11 shows the distribution of the deviatoric strain U_V defined by the third component of the formula (3). Comparison of the plots of Fig. 10 and 11 allows to state that the distributions of deviatoric strains are equal to inverses of distributions of non-deviatoric strains. In boundary elements of the surface layer the values of the volumetric strain energy are very small. Meanwhile,

the highest values occur in the elements located nearer to the inner free surface of the ring, in the locations where the density of the volumetric strain energy approximates zero.
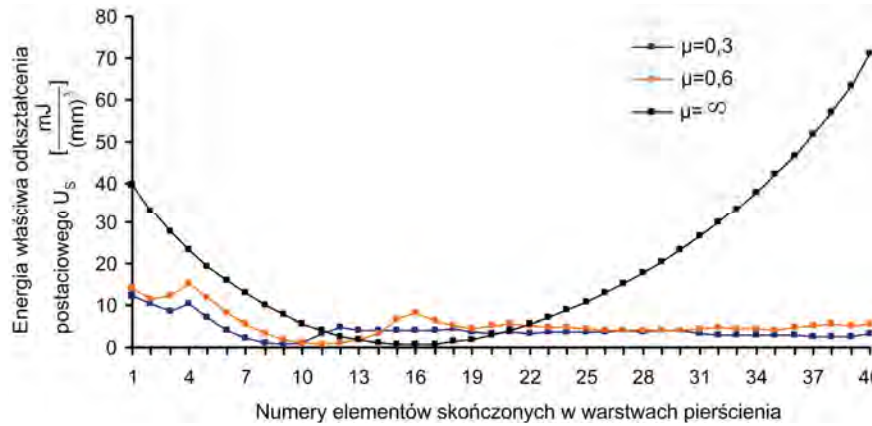

Fig. 10. Distribution of deviatoric strain energy density in the surface layer under plate
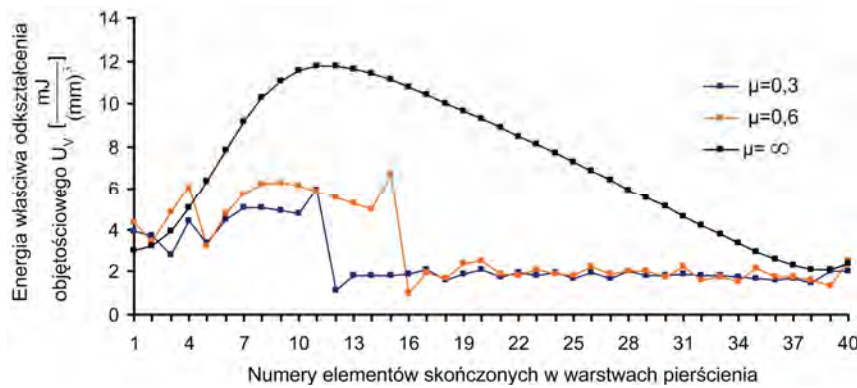

Fig. 11. Distribution of volumetric strain energy density in the surface layer under plate

Possible free displacement of the ring elements in the vicinity of the rubbing surface causes that even in case of large ring deflection the change in their total volume remains relatively small. Nevertheless, the elements located nearer the middle of the ring cross-section cannot displace as freely as the ones located nearer its free surfaces. Their displacement is constrained by the sum of the friction forces exerted by the surface elements of the surrounding material. This causes that the finite elements inside the cross-section are more compressed than the ones located nearer the ring free surfaces. Therefore, the change in their volume with respect to its initial value is higher and, in result, the volumetric strain energy cumulates in these elements.

Density of the strain energy U (Fig. 12) is defined by the formula (3). It is a sum of two formerly presented energy components: the density of deviatoric strain energy U_S and the density of volumetric strain energy U_V. Analysis of the plots of Fig. 12 enables finding that they are very similar to the U_S plots shown in Fig. 10. However, important difference between them consists in the fact that value of the energy U of the middle finite elements significantly exceeds the energy U_S. This is confirmation of the assumption adopted in the beginning that computation should take into account the volumetric strain of the material, since in spite of the fact that volumetric strain of a nearly incompressible material as rubber is small as compared to the deviatoric strain, its effect on final results remains significant.

One more fact deserves reader's attention. The value of strain energy in boundary finite elements located nearer the outer free surface of the ring, the nodes of which placed in the contact surface were locked, is nearly twenty times as large as in case of the ring with the friction coefficient in the plate-ring surface amounting to $\mu = 0.3$.
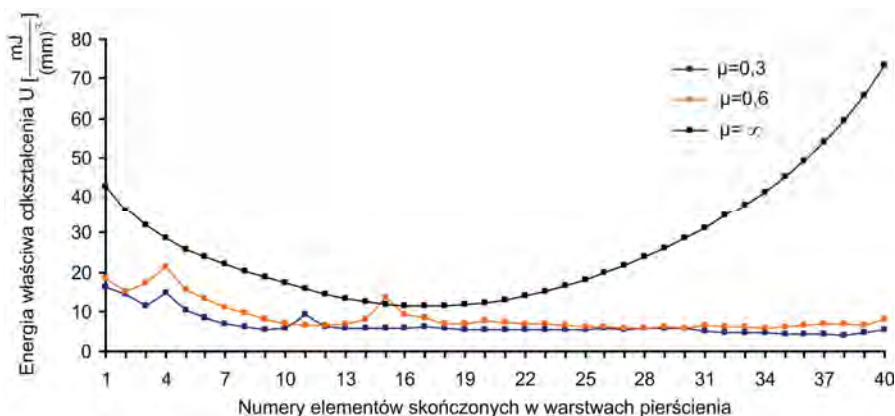
Fig. 12. Distribution of strain energy density in the surface layer under plate

6. Conclusions

Results of the computation confirm that the surface friction phenomenon significantly affects the ring strain. The factor that significantly affects the friction phenomenon is the value of the friction μ coefficients. It depends on the plate material and the outer factors that cause its variations, as, for example, the use of lubricants. Assumption of various friction coefficients caused that the shapes obtained after the deflection of $f = 1.5$ mm significantly differed each from other. The number of displaced nodes and the value of these displacements affected the final ring shape determining the ring strain condition and the distribution of the deviatoric energy and internal stress of the material. This indicates that the phenomenon of surface friction is very important taking the strength into account.

The ring deformation depends on friction intensity while the friction process depends, in turn, on the ring deformation. Hence, the above presented analysis indicates that for correct description of the friction phenomenon the material deformability of the body subject to friction must be considered.

References

[1] Bieliński, D., Dobrowolski, O., Głąb, P., Ślusarski, L., *Dyspersja napełniacza a właściwości tribologiczne i mechaniczne gumy*, Wydawnictwo Instytutu Technologii Eksploatacji – PIB, Tribologia Nr 4, s. 1081-1088, Radom 2002.
[2] Bowden, F. P., Tabor, D., *Wprowadzenie do trybologii*, WNT, Warszawa 1980.
[3] Hang, S., Hodgson, P. D., Cardew-Hall, M. J., Kalyanasundaram, S., *A finite element simulation of micro-mechanical frictional behaviour in metal forming*, Journal of Materials Processing Technology 134, pp. 81-91, 2003.
[4] Hebda, M., Wachal, A., *Trybologia*, WNT, Warszawa 1980.
[5] Jerrams, S.J., *Friction and adhesion in rigid surface indentation of nitrile rubber*, Materials and Design, 26, pp. 251-258, 2005.
[6] Marczak, K., *Warstwa wierzchnia. Współczesny stan wiedzy i kierunki przysz łych badań*, Wydawnictwo Instytutu Technologii Eksploatacji - PIB, Tribologia, Nr 3, s. 939-953, Radom 2002.
[7] Persson, B.N.J., Volokitin, A.I., *Rubber friction on smooth surfaces*, The European Physical Journal E 21, pp. 69-80, 2006.
[8] Wegner, T., *Energetyczna metoda modelowania i wyznaczania charakterystyk dynamicznych elementów mechanicznych o silnym t łumieniu*, Seria Rozprawy Nr 323, Wydawnictwo Politechniki Poznańskiej, 115 s., Poznań 1997.

[9] Wegner, T., *Analiza porównawcza zakresu stosowalno ści nieliniowych modeli materia łów ściśliwych*, Studia i Materiały XLVIII, seria Technika, Wydawnictwo Wyższej Szkoły Pedagogicznej, Z. 1, s. 159-173, Zielona Góra 1999.

[10] Wegner, T., *Metody energetyczne w wytrzyma łości materiałów Hipoteza wytrzymałościowa stateczności równowagi wew nętrznej*, Wydawnictwo Politechniki Poznańskiej, 81 s., Poznań 1999.

[11] Wegner, T., *Surface of limit state in nonlinear material and its relation with plasticit y condition*, The Archive of Mechanical Engineering, PAN, Vol. XLVII, No. 3, 2000, p. 205-223, Warszawa 2000.

[12] Wegner, T., *A method of materia l modelling w ith the use of streng th hypothesis of inner equilibrium stability*, Mechanics and Mechanical Engineering - International Journal, Vol. 4, No. 2, pp. 139-147, Łódź 2000.

[13] Wegner, T., *Zastosowanie metody relaksacji lokalnej do analizy zagadnie ń uwzględniających zjawisko tarcia powierzchniowego*, Zeszyty Naukowe Politechniki Poznańskiej, Seria Mechanika, Wydawnictwo Politechniki Poznańskiej, Nr 47, s. 73-87, Poznań 2000.

[14] Wegner, T., *Metoda energetyczna i Newtona-Raphsona w obliczeniach wytrzyma łościowych nieliniowych konstrukcji pr ętowych*, Zeszyty Naukowe Politechniki Poznańskiej, seria Mechanika, Wydawnictwo Politechniki Poznańskiej, Nr 47, s. 63-71, Poznań 2000.

[15] Wegner, T., *Matematyczne modelowanie mech anicznych właściwości materiałów*, Biuletyn WAT, Vol. LIV, Nr 12, s. 5-51, Warszawa 2005.

[16] Wegner, T., *Energetyczne modelowanie w nieliniowej mechanice materia łów i konstrukcji*, Wydawnictwo Politechniki Poznańskiej, 142 s., Poznań 2009.

[17] Wegner, T., Magnucki, K., Wasilewicz, P., *Large axisymmetrical deformation of a compressed ring made of a incompressible nonlinear material*, Mathematical Methods in Engineering, The conference with Foreign Participation, pp. 425-431, Karlovy Vary 1986.

[18] Wegner, T., Magnucki, K., Wasilewicz, P., *Finite deformation of nonlinearly elastic ring,* Engineering Transactions, PAN IPPT, 35, 4, pp. 695-704, Warszawa 1987.

[19] Wegner, T., Magnucki, K., Wasilewicz, P, *Compression of a ring to large deformations with dissipation of energy*, Archive of Applied Mechanics – Ingenieur-Archiv, 58, pp. 109-112, Springer-Verlag 1988.

[20] Wegner, T., Kokot, M., *Zastosowanie metody relaksacji lokalnej do analizy odkszta łceń pierścienia uwzględniającej zjawisko tarcia powierzchniow ego*, XX DIDMATTECH, T. 1, s. 256-263, Olomouc, Czechy 2007.

[21] Wegner, T., Kokot, M., *Wpływ zjawiska tarcia powierzchniowego na odkształcenia gumowego pierścienia*, Przegląd mechaniczny, LXVII, Z. 5/2008, s. 13-18, Warszawa 2008.

[22] Wegner, T., Pęczak, A., *Badanie zbieżności i dok ładności iteracyjnej p rocedury relaksacji lokalnej energetycznego elementu skończonego*, Materiały Konferencyjne IX Konferencji Naukowo Technicznej MES 2009, Programy MES w komputerowym wspomaganiu analizy, projektowania i wytwarzania, s. 113-120, Giżycko 2005.

[23] Wegner, T., Pęczak, A., *Metoda elementów sko ńczonych modelowanych ener getycznie*, Monografia pt. Analizy numeryczne wybranych zagadnień mechaniki (red. T. Niezgoda), R. 3, s. 59-83, Warszawa 2007.

[24] Wegner, T., Pęczak, A., *Rozszerzenie obiektowo zorientowanej metody elementów skończonych o koncepcję elementów sko ńczonych modelowanych energetycznie*, Acta mechanica et automatica, Vol. 2, No. 1, s. 81-90, Białystok 2008.

[25] Wegner, T., Pęczak, A., *Implementation of a strain energy-based nonlinear finite element in the object-oriented environment*, Computer Physics Communications, 181, pp. 520-531, Elsevier 2010, ScienceDirect: http://dx.doi.org/10.1016/j.cpc.2009.10.027.